Opt Quant Electron (2009) 41:513–523
DOI 10.1007/s11082-009-9352-8

Femtosecond pulse shaping using counter-propagating pulses in a semiconductor optical amplifier

Mohammad Razaghi · Vahid Ahmadi · Michael J. Connelly

Received: 6 October 2009 / Accepted: 1 December 2009 / Published online: 22 December 2009

Abstract An efficient pulse shaping method using counter-propagating pulses in the femtosecond regime is proposed and investigated. The effects of pump pulse power and pulsewidth on probe pulse are studied in counter-propagation scheme. It is shown that, with the proposed method, output probe pulse temporal and spectral peak shift due to femtosecond nonlinearities can be compensated, while the output pulse is amplified sufficiently. Furthermore, in relatively high power regime, the probe pulsewidth and time-bandwidth product are improved using counter-propagating pump pulse.

Keywords Semiconductor optical amplifiers · Nonlinear optical devices · Ultrafast nonlinear optics · Pulse shaping

1 Introduction

SOAs have unique features that make them an essential part of all-optical pulse shaping (AOPS) schemes Connelly (2002). In addition to their compact size, high optical efficiency and integrating to other optical devices, nonlinear properties of SOA play an important role in AOPS schemes Kang et al. (2008). Several schemes have been proposed for achieving proper AOPS. Some of these methods investigate AOPS of picosecond pulses by

M. Razaghi (✉)
Department of Electrical and Computer Engineering, University of Kurdistan,
P.O. Box 416, Sanandaj, Iran
e-mail: m.razaghi@uok.ac.ir

V. Ahmadi
Department of Electrical Engineering, Tarbiat Modares University, P.O. Box 14115-143,
Tehran, Iran
e-mail: v_ahmadi@modares.ac.ir

M. J. Connelly
Optical Communication Research group, Department of Electronic and Computer Engineering,
University of Limerick, Limerick, Ireland
e-mail: michael.connelly@ul.ie

using SOA in co-propagation Tang and Shore (1999), Gutiérrez-Castrejón and Duelk (2006) and counter-propagation schemes Fernandez et al. (2006), Chi et al. (2001). However, they have not included all nonlinear effects relevant to sub-picosecond regime. In some cases additional optical devices e.g. saturation absorber accompany SOA to achieve proper pulse shape Heck et al. (2007, 2008). The main stress of these works is on experimental results without a comprehensive model for their proposed scheme.

In sub-picosecond co-propagation scheme, the output pulses spectra are mixed so that probe pulse shape can hardly be distinguishable. To solve the problem, we propose an alternative method using a counter propagation scheme of SOA. Based on the scheme proposed here, SOA can be used for a multi-functional purpose. We illustrate how ultra-short output pulse shape and spectrum can be changed by the pump pulsewidth and power, while it is amplified due to intrinsic property of SOA.

To model the SOA in femtosecond regime, besides self phase modulation (SPM), it is essential to take into account nonlinear processes such as two-photon absorption (TPA), with dependency to carrier depletion, carrier heating (CH), spectral-hole burning (SHB) and their dispersion including the recovery time in SOA. In order to get an accurate model in this regime group velocity dispersion (GVD), gain dispersion and ultrafast nonlinear refraction (UNR) should be also included in the model. Several models have been proposed to analyze the counter pulse propagation in SOA in both frequency and time domain Fernandez et al. (2006), Occhi et al. (2003), Kim et al. (1999), Bischoff et al. (1999). To our knowledge none of these counter-propagating models include all the mentioned nonlinear effects simultaneously in sub-picosecond regime which leads to inaccurate results in both time and spectral domain. Therefore, their results can not exactly illustrate the leading and trailing edges of output pulse spectrum as obtained in experimental results, moreover the estimated net-gain value is considerably larger Razaghi et al. (2009), Hong et al. (1996). In contrast, because of inclusion of all nonlinear effects in our model, it agrees much better with the experimental results in sub-picosecond regime.

In this paper, using a numerical model we investigate, for the first time the effects of pump pulse on chirped probe pulse in femtosecond regime based on an improved finite difference beam propagation method (IFDBPM) Razaghi et al. (2009). It is shown that output probe pulse peak position can be controlled by pump pulse power and pulsewidth. For particular pump pulse powers, pulsewidths and time delays it is possible to decrease the amplified probe pulsewidth to half of its input value. Besides time-bandwidth product (TBP) of output probe pulse is improved significantly.

The analysis is based on a modified nonlinear Schrödinger equation (MNLSE) considering GVD, inter-band gain dynamics, inter-band refractive index dynamics, TPA, with carrier depletion consideration, UNR, CH, SHB, their dispersions and gain dispersion in an SOA. We also consider the gain peak shift with carrier density.

This paper is organized as follows. In the next section we introduce the theory and modeling scheme. In Sect. 3 we present simulation results. Conclusions are presented in Sect. 4.

2 Theory of the model

The counter-propagation MNLSE which describes the propagation of forward and backward optical field is given by Razaghi et al. (2009) :

$$\left[\pm\frac{\partial}{\partial z}+\frac{1}{v_g}\frac{\partial}{\partial t}\right]A^{\pm}(z,t)=\left\{\frac{i}{2}\beta_2\frac{\partial^2}{\partial t^2}-\left(\frac{\gamma_{2p}}{2}+ib_2\right)I(z,t)\right.$$

$$-\frac{\gamma}{2}+\frac{1}{2}g_N(t)\left[\frac{1}{f_T(t)}+i\alpha_N\right]+\frac{1}{2}\Delta g_T(t)\left[1+i\alpha_T\right]$$
$$-i\frac{1}{2}\left.\frac{\partial g(t,\omega)}{\partial\omega}\right|_{\omega_0}\frac{\partial}{\partial t}-\frac{1}{4}\left.\frac{\partial^2 g(t,\omega)}{\partial\omega^2}\right|_{\omega_0}\frac{\partial^2}{\partial t^2}\Bigg\}A^{\pm}(z,t) \tag{1}$$

where

$$g_N(t)=g_0\exp\left(-\frac{1}{W_s}\int_{-\infty}^{+\infty}U(s)e^{-s/\tau_s}I(z,t)ds\right) \tag{2}$$

$$\Delta g_T(t)=-h_1\int_{-\infty}^{+\infty}U(s)e^{-s/\tau_{ch}}\left(1-e^{-s/\tau_{shb}}\right)I(z,t)ds$$
$$-h_2\int_{-\infty}^{+\infty}U(s)e^{-s/\tau_{ch}}\left(1-e^{-s/\tau_{shb}}\right)I'(z,t)ds \tag{3}$$

$$f_T(t)=1+\frac{1}{\tau_{shb}P_{shb}}\int_{-\infty}^{+\infty}U(s)e^{-s/\tau_{shb}}I(z,t)ds \tag{4}$$

$$\left.\frac{\partial g(t,\omega)}{\partial\omega}\right|_{\omega_0}=A_1+B_1\left[g_0-g(t,\omega_0)\right] \tag{5}$$

$$\left.\frac{\partial^2 g(t,\omega)}{\partial\omega^2}\right|_{\omega_0}=A_2+B_2\left[g_0-g(t,\omega_0)\right] \tag{6}$$

$$g(t,\omega_0)=\frac{g_N(t,\omega_0)}{f_T(t)}+\Delta g_T(t,\omega_0). \tag{7}$$

The slowly varying envelope approximation is used in (1), where $A^+(z,t)$, $A^-(z,t)$ are the forward and backward time domain complex envelope function of an optical pulse, $I(z,t)$ is photon density given by $I(z,t)=|A^+(z,t)|^2+|A^-(z,t)|^2$ and $I'(z,t)=|A^+(z,t)|^4+|A^-(z,t)|^4$, β_2 is the GVD coefficient and v_g is the group velocity at transparency. γ is the linear loss, $b_2(=\omega_0 n_2/cA_r)$ is the instantaneous self-phase modulation term due to the UNR, n_2 is the Kerr effect coefficient, ω_0 is the center angular frequency of the pulse, c is the velocity of light in vacuum, $A_r(=wd/\Gamma)$ is the effective area (d and w are the thickness and width of the active region, respectively, and Γ is the confinement factor). $g_N(t)$ is the saturated gain due to carrier depletion, g_0 is the linear gain, W_s is the saturation energy, τ_s is the carrier lifetime, $f_T(t)$ is the SHB function, P_{shb} is the SHB saturation power, τ_{shb} is the SHB relaxation time, and α_N and α_T are the linewidth enhancement factor associated with the gain change due to carrier depletion and CH respectively. $\Delta g_T(t)$ is the resulting gain change due to the CH and TPA, $U(s)$ is the unit step function, τ_{ch} is the CH relaxation time. γ_{2p}, h_1 and h_2 are phenomenological constants including the strength of TPA, the contribution of stimulated emission (SE) and free carrier absorption (FCA) to CH included gain reduction and the contribution of TPA, respectively, Hong et al. (1996). Finally A_1 and A_2 are the slope and the curvature of the linear gain at ω_0, respectively, while B_1 and B_2 are constants describing changes in these quantities with saturation Hong et al. (1994).

For solving (1) we used IFDBPM Razaghi et al. (2009). In this method new parameter T defined as $v_g t$ is substituted in (1). Furthermore, propagation equations are solved by central

differentiation and trapezoidal integration techniques over a small step size Δ in new frame which is rotated to (z,T) coordinates by $-45°$. Δ is defined as L/M where L is the SOA length and M is number of sections. In following equations, two integers (m,N) are used instead of (z,T) so that $A(m,N)$ signifies $A(z = m\Delta, T = N\Delta)$. Finally the counter-propagation MNLSE based on IFDBPM scheme becomes:

$$\begin{aligned}
&-a^{+}(m+1,N+1)\times A^{+}(m+1,N)+\left[1-b^{+}(m+1,N+1)\right]\times A^{+}(m+1,N+1)\\
&\quad -c^{+}(m+1,N+1)\times A^{+}(m+1,N+2)=-a^{+}(m,N)\times A^{+}(m,N-1)\\
&\quad +\left[1-b^{+}(m,N)\right]\times A^{+}(m,N)-c^{+}(m,N)\times A^{+}(m,N+1) \qquad (8)\\
&-a^{-}(m+1,N+1)\times A^{-}(m+1,N)+\left[1-b^{-}(m+1,N+1)\right]\times A^{-}(m+1,N+1)\\
&\quad -c^{-}(m+1,N+1)\times A^{-}(m+1,N+2)=-a^{-}(m+2,N+2)\\
&\quad \times A^{-}(m+2,N+1)+\left[1-b^{-}(m+2,N+2)\right]\times A^{-}(m+2,N+2)\\
&\quad -c^{-}(m+2,N+2)\times A^{-}(m+2,N+3) \qquad (9)
\end{aligned}$$

where

$$a^{\pm}(m,N)=\frac{\Delta}{2}\left[\frac{i v_g^2\beta_2}{2\Delta^2}+\frac{i v_g}{4\Delta}\left.\frac{\partial g(N,\omega)}{\partial\omega}\right|_{\omega_0}-\frac{v_g^2}{4\Delta^2}\left.\frac{\partial^2 g(N,\omega)}{\partial\omega^2}\right|_{\omega_0}\right] \qquad (10)$$

$$\begin{aligned}
b^{\pm}(m,N)=-\frac{\Delta}{2}\Bigg[&\frac{i v_g^2\beta_2}{\Delta^2}+\frac{\gamma}{2}+v_g\left(\frac{\gamma_{2p}}{2}+ib_2\right)I(m,N)-\frac{v_g^2}{2\Delta^2}\left.\frac{\partial^2 g(N,\omega)}{\partial\omega^2}\right|_{\omega_0}\\
&+\frac{1}{2}\Delta g_T(N,\omega_0)\left[1+i\alpha_T\right]-\frac{1}{2}g_N(N,\omega_0)\left[\frac{1}{f_T(N)}+i\alpha_N\right]\Bigg] \qquad (11)
\end{aligned}$$

$$c^{\pm}(m,N)=\frac{\Delta}{2}\left[\frac{i v_g^2\beta_2}{2\Delta^2}-\frac{i v_g}{4\Delta}\left.\frac{\partial g(N,\omega)}{\partial\omega}\right|_{\omega_0}-\frac{v_g^2}{4\Delta^2}\left.\frac{\partial^2 g(N,\omega)}{\partial\omega^2}\right|_{\omega_0}\right] \qquad (12)$$

The accurate results can be obtained using iterative procedure described in Razaghi et al. (2009).

It is found that good convergence with $M = 384$ can be achieved if the input pulsewidth becomes 500 ps, but as the pulsewidth decreases more, M must be increased (e.g. $M = 512$ for 300 fs input pulsewidth).

3 Simulation results

The model results are verified in our past work Razaghi et al. (2009) by comparing with experimental Hong et al. (1994, 1996) and theoretical models Fernandez et al. (2006), Agrawal and Olsson (1989), Das et al. (2000) results. The SOA used in this simulation was a state-of-the-art, high-power, AlGaAs/GaAs, double heterostructure, traveling wave amplifier, with gain guiding and angle stripe geometry. The simulation parameters are given in Table 1 Hong et al. (1996).

In following results the input pulses are sech^2 and Fourier transform limited. The unsaturated gain (G_0) is taken as 30 dB. To investigate counter pulse propagation, we consider a 500 fs probe pulsewidth. In the case of linearly chirped sech pulses, the incident complex amplitude can be written as Agrawal (2001):

$$A^{\pm}(0,t)=(E_{in}/(2t_0))^{1/2}\times \text{sec h}\left(-(t/t_0)\right)\times\exp\left(-iC/2\times(t/t_0)^2\right) \qquad (13)$$

Table 1 List of parameters used in simulation Hong et al. (1996)

Symbol	Quantity	Value
L	SOA length	500 μm
A_r	Effective area	5 μm^2
fo	Center frequency of the pulse	349 THz
g_o	Linear gain	92 cm^{-1}
β_2	Group velocity dispersion	0.05 ps^2 cm^{-1}
E_{sat}	Saturation energy	80 pJ
α_N	Linewidth enhancement factor due to the carrier depletion	3.1
α_T	Linewidth enhancement factor due to the carrier heating	2.0
h_1	The contribution of simulated emission and free carrier absorption to the carrier heating gain reduction	0.13$cm^{-2}pj^{-1}$
h_2	The contribution of two photon absorption	126 fs cm^{-1} pJ^{-2}
τ_s	Carrier lifetime	200 ps
τ_{ch}	Carrier heating relaxation time	700 fs
τ_{shb}	Spectral-hole burning relaxation time	60 fs
P_{shb}	Spectral-hole burning relaxation power	28.3 W
γ	Linear loss	11.5 cm^{-1}
n_2	Instantaneous nonlinear Kerr effect	−0.70 cm^2 TW^{-1}
γ_{2p}	Two photon absorption coefficient	1.1 cm^{-1} W^{-1}
A_1		0.15fsμm^{-1}
A_2	Parameters describing second order Taylor	−80 fs
B_1	expansion of the dynamically gain spectrum	−60 fs^2μm^{-1}
B_2		0 fs^2

where E_{in} is the input pulse energy, t_0 is related to input pulse full-width at half-maximum (FWHM) by $T_{FWHM} \approx 1.763 t_0$ and C is the chirp parameter.

3.1 Low power regime

Temporal and spectral shapes of short optical pulses as propagate through the SOA cavity become a function of nonlinear phenomena such as SPM, SHB, CH and TPA. A proper counter-propagating pump pulse can lead to improved output probe shape and spectrum. The effect of 16 pJ unchirped pump pulse on 1 fJ probe pulse is illustrated in Fig. 1. The input probe pulses are linearly chirped and the pump pulsewidth is 1 ps. The detuning frequency between pump and probe is assumed to be 0.5 THz. $\Delta\omega$ is the pump probe detuning

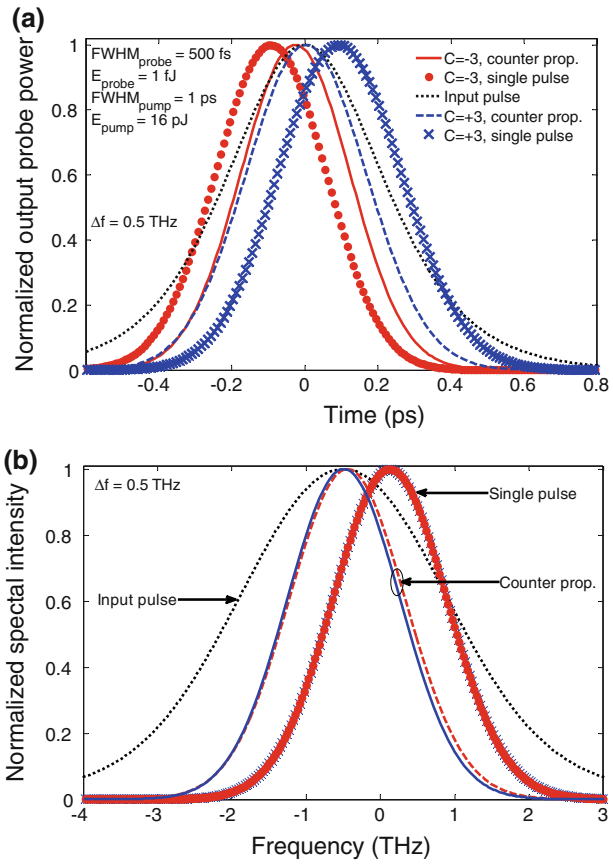

Fig. 1 **a** Normalized output probe shape for different energies of counter-propagating pump pulse and chirp parameters; **b** Normalized output probe spectrum for different energies of counter-propagating pump pulse and chirp parameters. The *colors and symbols* used here correspond to Fig. 1a

expressed as $\Delta\omega = 2\pi(f_{\text{pump}} - f_{\text{probe}})$ Das et al. (2000). As shown in Fig. 1a shows the output probe peak position can be shifted to its initial position in presence of pump pulse. The probe peak shifts from its initial position either to positive and negative values based on its initial chirp parameter (C), which results in distortion of propagated pulse shape. This is because of including the effect of SOA gain dispersion in our model. As can be observed the output probe pulse is also compressed by 30% from its initial value. In Fig. 1b the effect of pump pulse on chirped probe pulse spectrum is shown. Based on the results in the absence of pump pulse output probe peak is blue shifted. As it shows pump pulse can be used to compensate this shift for both positive and negative input probe chirp parameters. Besides the output probe spectrum is compressed to half of its input spectral width in this regime.

The effects of unchirped pump pulse energy on linearly chirped probe pulse for different chirp values and detuning frequencies are also investigated in Fig. 2a. As depicted in the figure, in the absence of pump pulse, output pulse peak shifts are +40 fs and −40 fs for input pulse chirp parameters of +3 and −3, respectively. The effect of detuning frequency is also shown in Fig. 2a. For low power probe pulses, in presence of detuning, GVD effects should not be neglected because the probe pulsewidth in femtosecond regime becomes smaller than

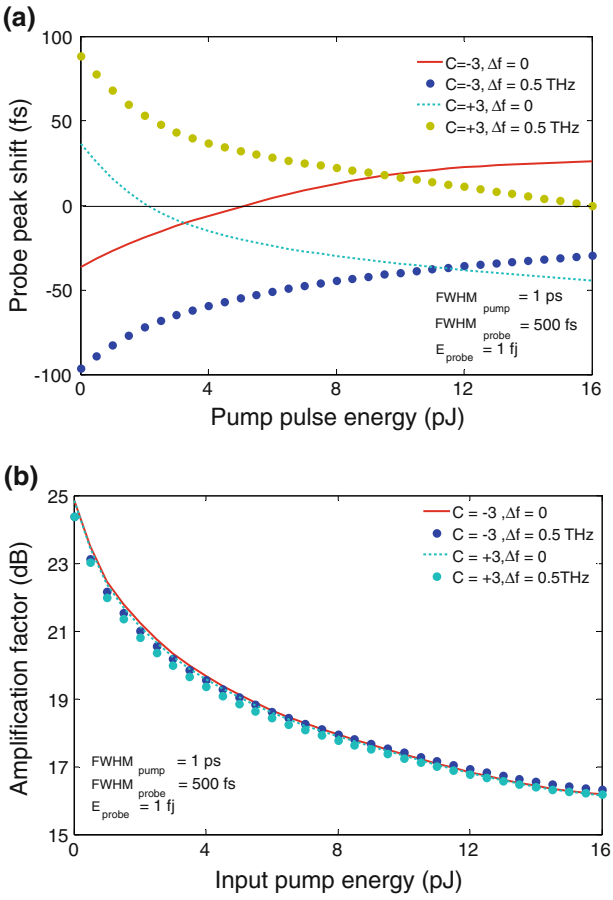

Fig. 2 **a** Probe peak shift versus input pump pulse power for different chirped input pulses and detuning frequencies; **b** Amplification factor versus input pump pulse power for different chirped input pulses and detuning frequencies

the pulse propagation time (7 ps for 500 μm waveguide). As detuning increases the effect of GVD becomes more important Das et al. (2000). This phenomenon increases the output pulse peak shift and so distorts the output pulse shape. Based on the results shown in Fig. 2a for the pulse with input chirp of 3 and detuning frequency of 0.5 THz, this peak shift in absence of pump pulse is become as large as 90 fs. This value is comparable with the pulse output pulsewidth which in this case is 350 fs. Injection of a pump pulse that is counter-propagating to the probe pulse can be used to reduce the probe pulse distortion. As shown in Fig. 2a for the probe pulses with +3 and −3 chirp and 0.5 THz detuning frequency using the 16 pJ pump energy can reset the probe pulse peak position to its initial value. On the other hand, the propagated pulse in this regime has an acceptable amplification factor (AF) as shown in Fig. 2b because of negligible SPM effect on low power probe pulse. The AF is defined as the ratio of output probe pulse energy to input probe pulse energy. These features in counter-propagation scheme can be used for efficient pulse reshaping purpose for distorted input pulses.

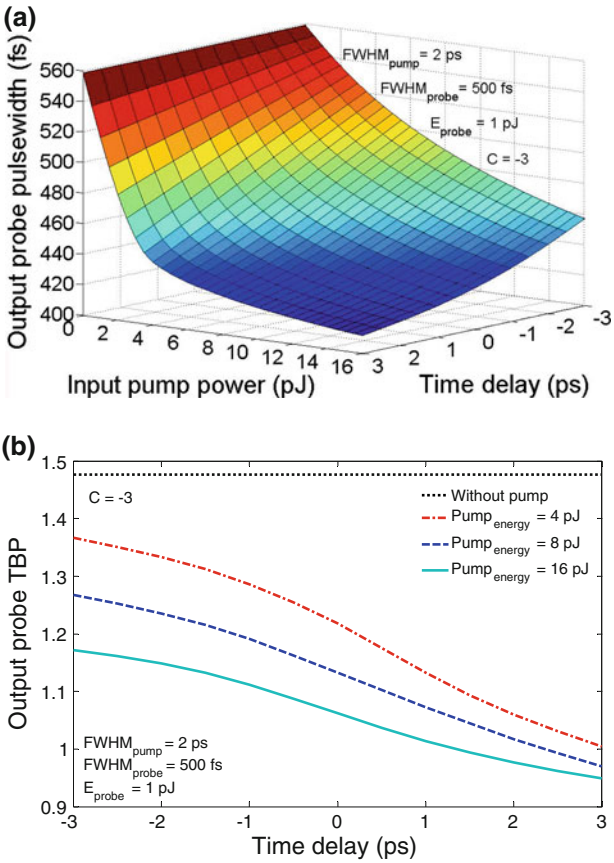

Fig. 3 **a** Output probe pulsewidth as a function of time delay between pump and probe pulses for several input pump pulse energies; **b** Output probe pulsewidth as a function of time delay between pump and probe pulses for several input pump pulse energies

3.2 High power regime

It should be noted that SPM is only negligible in low power regime. As the input probe pulse power increases SPM effect becomes more important and broadens the probe pulse. Counter propagating pump pulse can be used to compress both the temporal and spectral shapes of the probe pulse. The effect of pump pulse on probe pulse is investigated in this regime by setting the input probe energy to 1 pJ. Figure 3a shows the output probe pulsewidth versus time delay between probe and pump pulse for different pump pulse energies. Negative and positive time delay means that the probe pulse is injected to the SOA before and after the pump pulse, respectively. It shows that for greater positive time delays we have larger compression factor and consequently shorter output probe pulse. This is because for negative time delays when probe pulse is injected before the pump pulse, carrier depletion caused by overall nonlinear phenomenon such as SPM, CH, TPA affects a part of propagated probe pulse and a portion of probe pulse can propagate through the cavity without sensing any nonlinear effects and is amplified linearly. But for positive time delays, as the pump pulse is injected before the probe pulse, the variation of carrier density caused by the nonlinearities affects entire propa-

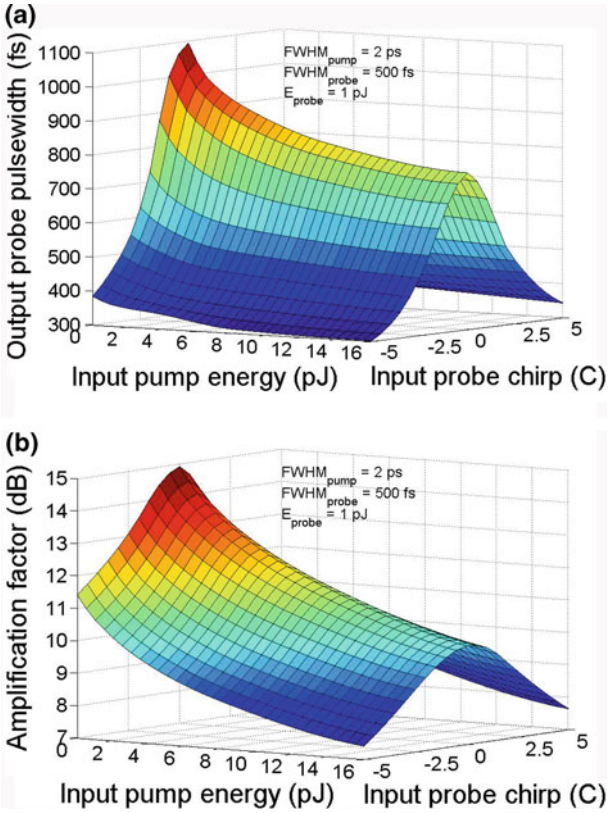

Fig. 4 **a** Output probe pulsewidth versus input pump energy for 2 ps input pump pulsewidth; **b** Amplification factor versus input pump energy for 2 ps input pump pulsewidth

gated probe pulse shape which becomes more crucial compared with the negative time delay. In this case, especially fast process nonlinearities such as CH and TPA make much more suppression on the propagated pulse. In fact the cross-phase modulation (XPM) included in model represents the nonlinear effect of gain saturation mechanism induced by high-power pump pulse.

The effect of time delay on output probe time-bandwidth product (TBP) is illustrated in Fig. 3b. It shows that TBP improves for higher input pump pulse energies. Based on the results, in high power regime, counter propagating pump pulse improves both output probe pulsewidth and TBP. Besides, time delay between pump and probe pulses play an important role to control characteristics of output probe pulse such as pulsewidth and TBP.

The effects of input pump pulse power on output probe pulsewidth for different input chirp parameters are shown in Fig. 4a. The counter propagating input pump and probe pulses are injected into the SOA simultaneously. As the pump pulse energy increased the effect of carrier depletion effects caused by SHB phenomenon increased on propagated probe pulse. Furthermore according to the results, the probe pulse is compressed for all the values of input probe chirp. We can define compression factor C_f as $(W_{p0} - W_{\text{pmax}})/W_{p0}$, where W_{p0} and W_{pmax} are the output probe pulsewidth without pump pulse and with maximum pump pulse energy, respectively. Based on the results shown in Fig. 4a, C_f is equal to 0.47 for the

unchirped probe pulse, while it is 0.27 and 0.19 for probe pulses with the initial chirps of 5 and −5, respectively. For further pulse compression, time detuning between pump and probe pulse can be used as described in Fig. 3a.

Although increasing the pump pulsewidth leads to better pulse compression, it should be noted that this increment for high power pump pulses, decreases the amplification factor of probe pulse as shown in Fig. 4b. Thus for efficient pulse compression and amplification, pump pulsewidth parameter should be chosen carefully.

4 Conclusion

Counter pulse propagation in semiconductor optical amplifier was studied in this paper for femtosecond pulse shaping. It was shown that in low power regime, with counter-propagation scheme output probe peak shift for different probe chirp and detuning frequencies can be compensated, while at the same time the output probe pulse was amplified sufficiently. Furthermore, simultaneously output probe spectral peak position can be also shifted to its initial value. The effects of counter-propagating pump pulse, on probe pulse shape and spectrum in relatively high power regime were also discussed. It was shown that time delays between pump and probe increase output pulse compression and simultaneously improve the output probe TBP. The effect of chirp parameter was also studied on output probe pulsewidth and amplification factor. As it was depicted, pump power, pulsewidth and time delay from input probe pulse, play an important role for efficient pulse shaping and reshaping purpose.

Acknowledgments This work was supported in part by Iran Telecommunication Research Center (ITRC) under the grant T/500/8482.

References

Agrawal, G.P.: Nonlinear Fiber Optics, 3rd ed. Academic Press, New York (2001)

Agrawal, G.P., Olsson, N.A.: Self-phase modulation and spectral broadening of optical pulses in semiconductor laser amplifiers. IEEE J. Quantum Electron. **25**(11), 2297–2306 (1989)

Bischoff, S., Buxens, A., Poulsen, H.N., Clausen, A.T., Mørk, J.: Bidirectional four-wave mixing in semiconductor optical amplifiers: theory and experiment. J. Lightwave Technol. **17**(9), 1617–1625 (1999)

Chi, J.W.D., Lu, C., Rao, M.K.: Time-domain large-signal investigation on nonlinear interactions between an optical pulse and semiconductor waveguides. IEEE J. Quantum Electron. **37**(10), 1329–1336 (2001)

Connelly, M.J.: Semiconductor Optical Amplifiers. Kluwer, Boston: MA (2002)

Das, N.K., Yamayoshi, Y., Kawaguchi, H.: Analysis of basic four-wave mixing characteristics in a semiconductor optical amplifier by the finite-difference beam propagation method. IEEE J. Quantum Electron. **36**(10), 1184–1192 (2000)

Fernandez, A., Morel, P., Chi, J.W.D.: Temporal and spectral properties of contra-propagating picosecond optical pulses in SOA. Opt. Commun **259**(2), 465–469 (2006)

Gutiérrez-Castrejón, R., Duelk, M.: Uni-directional time-domain bulk SOA Simulator considering carrier depletion by amplified spontaneous emission. IEEE J. Quantum Electron **42**(6), 581–588 (2006)

Heck, M.J.R., Bente, E.A.J.M., Barbarin, Y., Fryda, A., Hyun-Do, J., Yok-Siang, O., Notzel, R., Lenstra, D., Smit, M.K.: Characterization of a monolithic concatenated SOA/SA waveguide device for picosecond pulse amplification and shaping. IEEE J. Quantum Electron. **44**(4), 360–369 (2008)

Heck, M.J.R., Bente, A.J.M., Barbarin, Y., Lenstra, D., Smit, M.K.: Monolithic semiconductor waveguide device concept for picosecond pulse amplification, isolation, and spectral shaping. IEEE J. Quantum Electron **43**(10), 910–922 (2007)

Hong, M.Y., Chang, Y.H., Dienes, A., Heritage, J.P., Delfyett, P.J., Dijaili, S., Patterson, F.G.: Femtosecond self- and cross-phase modulation in semiconductor laser amplifiers. IEEE J. Sel. Topics Quantum. Electron. **2**(3), 523–539 (1996)

Hong, M.Y., Chang, Y.H., Dienes, A., Heritage, J.P., Delfyett, P.J.: Subpicosecond pulse amplification in semiconductor laser amplifiers: theory and experiment. IEEE J. Quantum Electron. **30**(4), 1122–1131 (1994)

Kang, I., Dorrer, C., Liming, Z., Dinu, M., Rasras, M., Buhl, L.L., Cabot, S., Bhardwaj, A., Xiang, L., Cappuzzo, M.A., Gomez, L., Wong-Foy, A., Chen, Y.F., Dutta, N.K., Patel, S.S., Neilson, D.T., Giles, C.R., Piccirilli, A., Jaques, J.: Characterization of the dynamical processes in all-optical signal processing using semiconductor optical amplifiers. IEEE J. Sel. Topics Quantum. Electron **14**(3), 758–769 (2008)

Kim, Y., Lee, H., Kim, S., Ko, J., Jeong, J.: Analysis of frequency chirping and extinction ratio of optical phase conjugate signals by four-wave mixing in SOA's. IEEE J. Sel. Topics Quantum. Electron. **5**(3), 873–879 (1999)

Occhi, L., Schares, L., Guekos, G.: Phase modeling based on the α-factor in bulk semiconductor optical amplifiers. IEEE J. Sel. Topics Quantum. Electron. **9**(3), 788–797 (2003)

Razaghi, M., Ahmadi, V., Connelly, M.J.: Comprehensive finite-difference time-dependent beam propagation model of counterpropagating picosecond pulses in a semiconductor optical amplifier. J. Lightwave Technol. **27**(15), 3162–3174 (2009)

Tang, J.M., Shore, K.A.: Active picosecond optical pulse compression in semiconductor optical amplifiers. IEEE J. Quantum Electron **35**(1), 93–100 (1999)